SAE TECHNICAL PAPER SERIES

2002-01-1110

A Detailed Two-Dimensional Numerical Study of Spark Ignition Including Ionization

M. Thiele, S. Selle, U. Riedel and J. Warnatz
Interdisziplinäres Zentrum für Wissenschaftliches Rechnen (IWR)
Universität Heidelberg

R. Schießl and U. Maas
Institut für Technische Verbrennung,
Universität Stuttgart

Reprinted From: Modeling of SI Engines and Multi-Dimensional Engine Modeling (SP–1702)

The Engineering Society For Advancing Mobility Land Sea Air and Space®
INTERNATIONAL

SAE 2002 World Congress
Detroit, Michigan
March 4-7, 2002

400 Commonwealth Drive, Warrendale, PA 15096-0001 U.S.A. Tel: (724) 776-4841 Fax: (724) 776-5760

ISSN 0148-7191

Printed in USA

2002-01-1110

A Detailed Two-Dimensional Numerical Study of Spark Ignition Including Ionization

M. Thiele, S. Selle, U. Riedel[1] and J. Warnatz
Interdisziplinäres Zentrum für Wissenschaftliches Rechnen (IWR) Universität Heidelberg

R. Schießl and U. Maas
Institut für Technische Verbrennung, Universität Stuttgart

ABSTRACT

In this work, the spark–ignition (SI) of a methane/air mixture contained in a constant–volume chamber is investigated by numerical simulations. A cylinder–shaped vessel filled with a methane/air mixture containing two electrodes is used as simulation model. The impact of an electrical discharge at the electrodes on the surrounding gas is simulated, with detailed treatment of the ignition process involvig chemical kinetics, transport phenomena in the gas–phase and electrodynamical modeling of the interaction between spark and fuel/air mixture. For the calculations, a 2D–code to simulate the early stages of flame development, shortly after the breakdown discharge, has been developed. Computational results are shown for ignition of a methane air–mixture.

INTRODUCTION

Spark ignition is an important means to initiate combustion in technical systems, SI engines being the most widespread. Since the early days of SI–engine development, it was known that the design of the spark plug has great impact on the development of combustion and engine performance [9]. Nowadays, with increasing demands on fuel economy and always stricter limitations on pollutant emissions, spark ignition systems are still far from being fully developed. This is certainly not due to the lack of commercial or academic interest on the field (see e. g. [6, 7, 8, 10, 11, 13, 14]), but mainly due to the missing knowledge concerning the detailed physical and chemical processes taking place during spark ignition.

Better understanding of spark ignition is aggravated by the fact that many different processes occur simultaneously during ignition, and that these processes are mutually influencing themselves in a complicated fashion. With experimental investigations, it is often difficult to achieve the desired information about the ignition system. This is partly because many important quantities are hard to measure (e. g. the temperature or the chemical composition of the plasma in the spark), but also because it is often hard to distinguish the many different effects that occur simultaneously, making interpretation of measurements difficult.

In contrast, investigating the behaviour of ignition systems by means of computer–simulations offers attractive features: In simulation models, all parameters can be varied and their behaviour can be examined at will; it is easy to study the influence of one specific parameter to the system, without interference of other quantities. However, in order to perform realistic simulations, many computational, chemical and physical issues have to be regarded.

In an earlier paper [1] the various approaches to model SI have been summarized. In [2] a comparison of different models for the electrical source term in spark ignition has been presented. Validation of the submodels used in this study (see below) as well as a comparison of the flame kernel development for two different configurations, i. e. electrode geometry and energy input to the system, is addressed in [1].

MODEL DESCRIPTION

MATHEMATICAL MODEL In the calculations, we consider a cylindrical system as sketched in Fig. 1. The spark–plug is represented by two electrodes (cylindrical rods) with 45°–tips on the top. The domain is limited by rigid, insulating walls, rendering a disk–shaped chamber

*Corresponding author. Adress: Interdisziplinaeres Zentrum fuer Wissenschaftliches Rechnen (IWR), Universitaet Heidelberg, Im Neuenheimer Feld 368, D–69120 Heidelberg, Phone: +49.6221.54.8887, FAX: +49.6221.54.8884

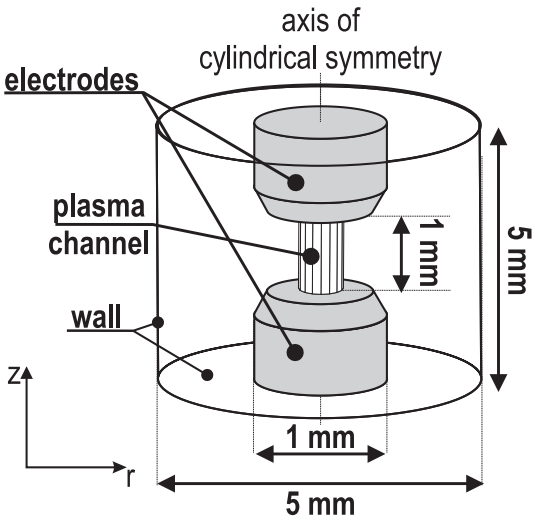

Figure 1: Sketch of the computational region (not to scale). The electrodes and surrounding walls are shown. Note the cylindrical symmetry around the electrode axes.

filled with a CH_4/air mixture. For the whole setup, cylindrical symmetry is assumed. This allows to treat a three–dimensional geometry by a two–dimensional calculation. The spark plasma channel formed by the breakdown is incorporated into the model as the initial condition [15].

Setting up an appropriate set of conservation equations for the reactive flow (see below), we assume that

- relaxation times of internal energy states of molecules are small compared to the time scales of the ignition process (*local thermal equilibrium assumption*).
- the electrodes have a uniform temperature distribution
- the influence of the magnetic field is negligible
- the plasma is transparent to its own radiation.
- no buoyancy effects are present

To describe the reactive flow, the complete compressible Navier–Stokes equations, together with chemical source terms and energy and species mass conservation are employed [16]. For the modeling of the chemical reactions, two mechanisms were considered:

MC1: A detailed reaction mechanism consisting of 15 species and 84 elementary reactions for a methane–air mixture.

MC2: An extended reaction scheme, obtained by augmenting MC1 by the 7 ions N_2^+, NO^+, N^+, O^+, H_3O^+, HCO^+, CO^+, and electrons (e^-) [19]. This results in a total of 118 elementary reactions of 23 species.

Because air is the main component of the mixture and only little data is available on ionization of methane, ions of CH_x–species are not considered in the reaction scheme.

To overcome the need of resolving the small length scales of shock–fronts (down to less than $1\ \mu$m), an artificial viscosity method was used that broadens the front without influencing the flow–field [1].

The resulting differential–algebraical equation system is discretized in time and space and then solved. Details of the solution procedure are outlined in [18].

TRANSPORT MODEL Molecular transport processes like diffusion or heat conduction can highly influence the behaviour of combustion systems. In our calculations, we use a transport model that is based on the theory of dilute gases by Chapman and Enskog (CE-theory) as described in detail in [3] or [4]. Appropriate potentials describing the interaction between neutrals, neutrals and charged particles (including resonant charge transfer) and between charged particles are considered as explained in detail in [5].

All species are considered in the transport properties of the mixture. A recent comparison between multicomponent formulations [5] has shown that the direct solution of the complete linear system is very time consuming compared to the first iterate in a conjugate gradient solution of the transport system [20]. However, both methods yield about the same accuracy of the results. Therefore, all computations were done using the approximations given in [20]. All transport coefficients are computed in the first approximation of CE–theory. The electro–dynamical model must be completed by an equation to derive the electrical conductivity σ. This quantity is derived from the ordinary diffusion coefficients. Heat loss from the gas phase into the electrodes is accounted for by introducing a gross transfer rate of 200 W/m^2. It has been shown that in the short time interval considered in our calculations, heat loss to the electrodes and by radiation is negligible [18].

ENERGY INPUT In the energy conservation equation the coupling with the electrodynamic equations is modeled by a source term $\dot{q}_e$, which accounts for energy deposition by the discharge due to resistive heating and is given by $\dot{q}_e = \sigma \cdot |\mathrm{grad}\,\Phi|$, where Φ is the potential and σ the conductivity, and assuming that the plasma is electrically neutral. The gradient of the potential can be obtained by a solution of Maxwell's equations [17]. Assuming that the medium is isotropically conducting, that Ohm's law is valid, that the field attains a quasi–steady state, and neglecting influences of the magnetic field, these equations can be reduced to the simple, time–independent equation $\mathrm{div}(-\sigma\,\mathrm{grad}\,\Phi) = 0$. Therefore, during this phase one can assume that electrical current flows in the z–direction only, i.e. the radial component of the electric field inside the kernel is much smaller than the axial component. Outside the channel the heating by the electric current is negligible due to vanishing conductivity. In this case, the Joule heat source can be determined directly from the total electrical

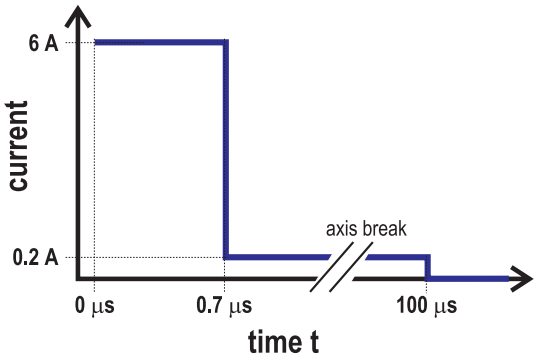

Figure 2: Example of a temporal profile of the electrical input current used in the calculations. Note the axis break.

current I [12, 13] by

$$\dot{q}_e = \sigma I^2 \left(\int_0^{R_c} 2\pi r \sigma(r,z)\,dr \right)^{-2} . \qquad (1)$$

In the calculations, the electrical source term is modeled by a temporal step–profile $I(t)$ of the input current. The current starts with a high value (typically 5...10 Ampere) at $t = 0$, and is reduced discontinually after a certain time to a much lower value (typically 0.2 Amperes). The values are given for each calculation below. As soon as the heated gas leaves the electrode gap the radial component of the electric field becomes more and more important, because the flame kernel develops a spherical shape. The assumption of a negligible radial field component is then no longer justified.

RESULTS

PRESSURE, FLOW FIELD, AND TEMPERATURE The results presented in this section were obtained with the following conditions: A lean methane/air mixture with $\lambda = 1.25$, initially at a pressure of $p = 8.5 \times 10^5$ Pa and a temperature $T = 300$ K. Chemical rate kinetics given by the MC2–mechanism, (118 reactions of 23 species, including 7 ions). The temporal step profile $I(t)$ for the current input was set to

$$I(t) = \begin{cases} 6\,\text{A} & \text{for} \quad 0 < t < 0.7\,\mu\text{s} \\ 0.2\,\text{A} & \text{for} \quad 0.7\,\mu\text{s} < t < 100\,\mu\text{s} \\ 0 & \text{for} \quad t > 100\,\mu\text{s} \end{cases} . \qquad (2)$$

Fig. 3 shows the resulting temporal development of the pressure– and velocity–field inside the modelled volume as a series of pictures (snapshots). Note that only the right half of a planar cut through the symmetry axis of the cylindrical volume is shown; due to the symmetry of the computational domain, this displays no loss of information. Each image is a pseudo–color plot of the pressure field. In the upper half, stream lines of the velocity field, and in the lower half, contour lines of the pressure are overlaid. The electrodes are indicated as white boxes on the left border. For each image, the corresponding false color code and the time are indicated.

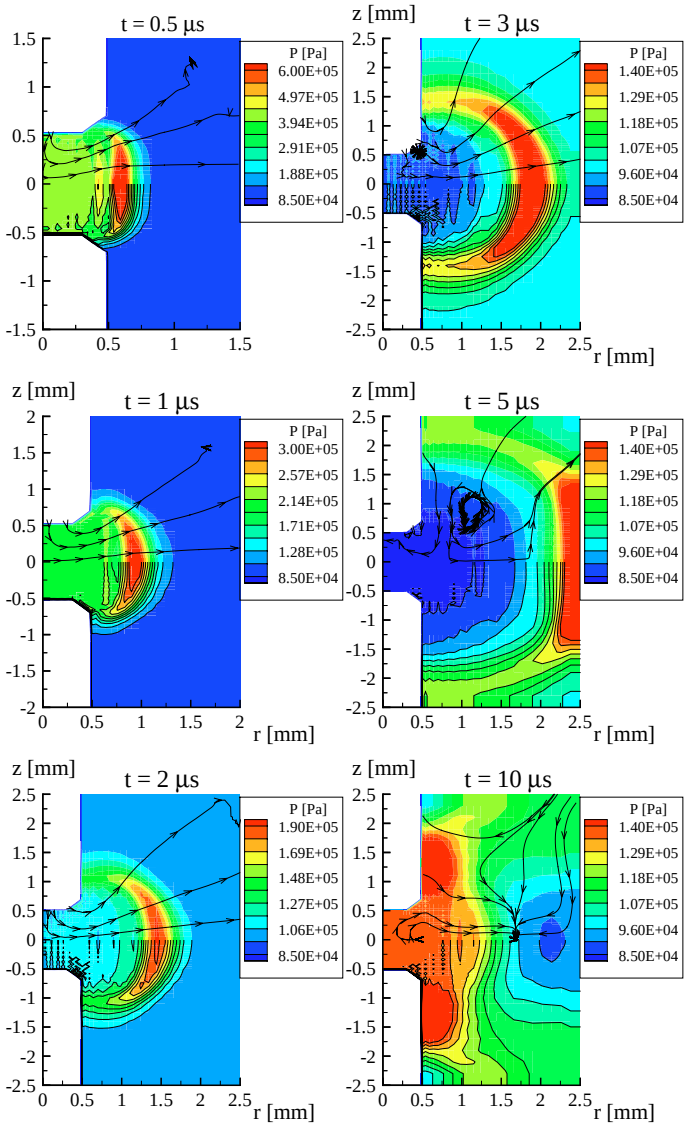

Figure 3: Contour lines of pressure at 0.5 μs, 1 μs, 2 μs, 3 μs, 5 μs, and 10 μs. In the upper part of each image, some streamlines of the gas velocity field are indicated.

During the breakdown phase, gas temperatures rise rapidly in a small channel between the electrodes. This causes the formation of a pressure wave that propagates from the electrode gap into the chamber. During the first 3 μs, the pressure maximum decreases significantly from $p_{max} \approx 6$ bar at $t = 0.5\,\mu$s to $p_{max} \approx 1.4$ bar. As can be seen from the steep gradients of the pressure field, a pressure wave is emitted from the electrodes, which is reflected at the wall at $t \approx 5\,\mu$s. At this time, a rarefaction wave behind the shock–front is clearly visible. The shock wave is reflected again at the electrodes after 10 μs. Interestingly, the velocity stream lines indicate that a vortex pair is formed after 3 μs at the edges of the electrodes, which is detaching and growing (vortex center at $r = 1.1$ mm, $z = 1$ mm after 5 μs).

Fig. 4 analogously displays the temperature field together with velocity streamlines in the lower half of each image at different times. The influence of the walls is clearly visible,

showing the flame kernel development for the first 50 μs. At 5 μs the gas is flowing inward into the electrode gap and is deflected to the side leading to the formation of a vortex pair which is disappearing after about 10 μs due to the changes of the local flow direction as a result of the reflection of the pressure wave.

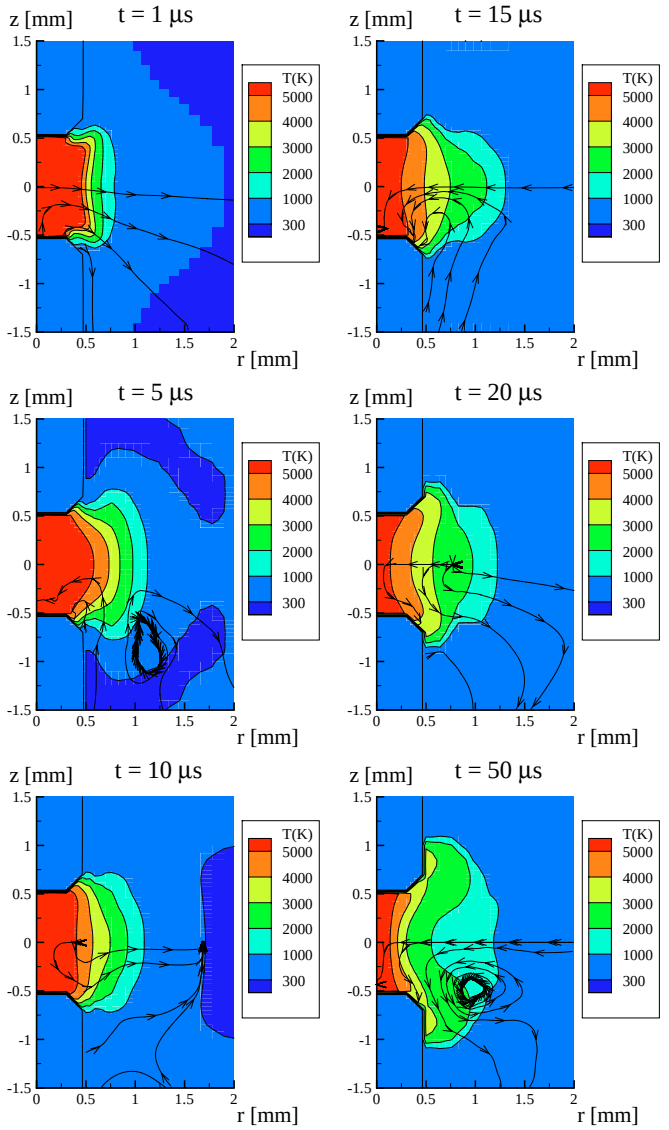

Figure 4: Flame kernel development (temperature contour lines) at 1 μs, 5 μs, 10 μs, 15 μs, 20 μs, and 50 μs. In the lower part of each image, some streamlines of the gas velocity field are indicated.

At 15 μs there is a strong interaction of flow field and shape of the flame kernel: The gas moving right to left is distorting the isolines into the direction of the cylinder axis. This effect gets even more pronounced at about 20 μs despite the fact that the flow direction is beginning to change.

At 50 μs the flow direction has changed several times and as a result the flame kernel is almost split into an upper and lower part. This is also the reason for the stagnating flame spread. The results reveal the significant influence of the walls that is impressed to the system by interaction with reflected pressure waves.

THE INFLUENCE OF IONS To assess the influence of ions in the reacting flow model in more detail, a new set of calculations was performed. A methane/air mixture at $\lambda = 1.25$ and the same geometry as in the previous calculations was considered. The temporal step profile $I(t)$ for the current input was set to

$$I(t) = \begin{cases} 6\,\mathrm{A} & \text{for} \quad 0 < t < 0.3\,\mu\mathrm{s} \\ 0.2\,\mathrm{A} & \text{for} \quad 0.3\,\mu\mathrm{s} < t < 100\,\mu\mathrm{s} \\ 0 & \text{for} \quad t > 100\,\mu\mathrm{s} \quad . \end{cases} \tag{3}$$

Two calculations were performed, based on the two different mechanisms (see above) MC1 (CH_4/air, no ions) and MC2 (CH_4/air, with ions).

Fig. 5 shows the temperature field after 1 μs, 10 μs, 25 μs, and 90 μs. After 1 μs, the high temperature region

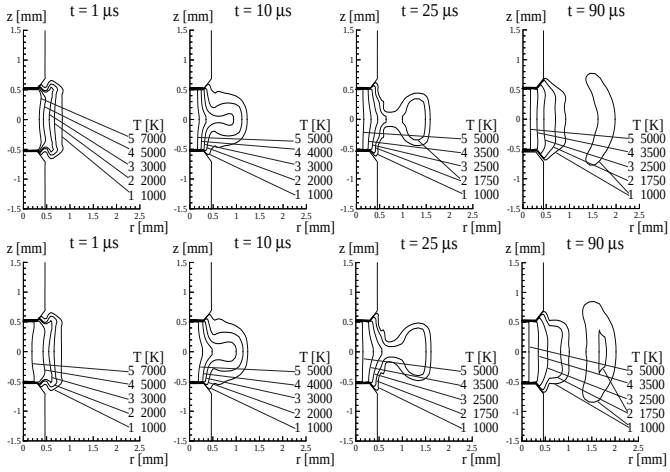

Figure 5: Isothermals of the temperature field at 1 μs, 10 μs, 25 μs, and 90 μs (left to right). Upper row: Without ions, lower row: With ions.

($T > 7000$ K) is considerably more extended when ion formation is neglected; also, the maximum temperatures are higher compared to a scheme with ions (MC2). The 1000 K to 5000 K–isothermals are similar for both mechanisms. At 10 μs the 3000 K and 4000 K isolines obtained when ions are regarded (MC2), indicate the effect of ion recombination: energetic ions are transported towards the electrodes' tip where they recombine leading to higher temperatures in that region. This effect increases in time, which can be seen by comparing the pictures for $t = 25\,\mu$s and $t = 90\,\mu$s, where the formation of a hot "pocket" can be seen. At 90 μs, this isolated hot pocket is present for both schemes, however with scheme MC2 a larger activated volume can be observed.

Fig. 6 compares radial temperature profiles, as obtained from calculations with the two different mechanisms MC1 and MC2, for the times $t = 1\,\mu$s, $t = 10\,\mu$s, $t = 25\,\mu$s,

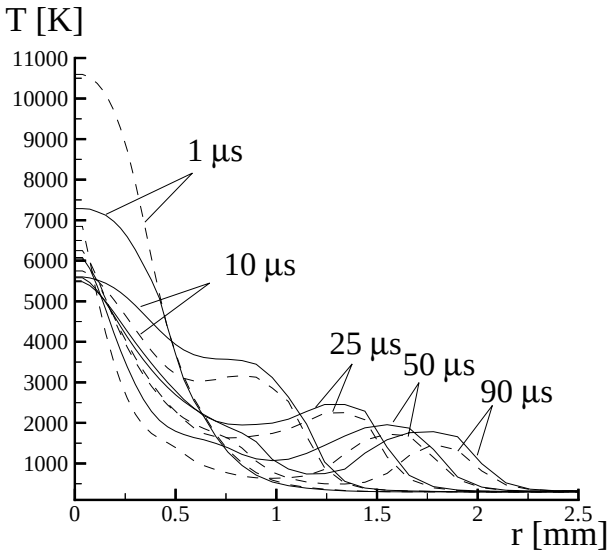

Figure 6: Radial temperature profile along the symmetry line between the electrodes for 1 μs, 10 μs, 25 μs, 50 μs, and 90 μs (line: With ions, broken line: Without ions). for a Methane/Air mixture (λ = 1.25).

$t = 50\,\mu s$ and $t = 90\,\mu s$. The profiles are taken from the centerline between the two electrodes. At $1\,\mu s$ the temperature is about 3000 K higher without ions (scheme MC1) compared to the calculation with ions. As stated above, this can be explained by the fact that there is considerable energy conversion by ionization. At $10\,\mu s$ and later times the difference gets smaller; scheme MC2 now leads to higher temperatures due to the energy released in ion recombination reactions.

After $25\,\mu s$ all profiles develop a local minimum corresponding to the pocket formation phenomenon shown in Fig. 5.

CONCLUSIONS

Based on a detailed model for the coupling of two–dimensional cylindrical reactive flows with electrodynamics, the early development of a stable flame kernel during spark ignition was investigated. Two–dimensional calculations of the spark–ignition in a cylindrical vessel filled with a lean methane/air mixture were undertaken using detailed CH_4/air reaction schemes and transport models.

Calculated 2D–fields of temperature, pressure and gas velocity are presented. The results display the generation of a pressure wave by the hot, expanding channel between the electrodes. The influence of this pressure wave on the temperature and velocity fields, as well as its interaction with rigid walls, is quite high and cannot be neglected if an appropriate description of the ignition process is required.

The effect of ions on the ignition process was assessed by comparing results of calculations with some ions regarded and with all ions neglected. It is demonstrated that, if ions are regarded in the chemical reaction scheme, a considerably different spatial and temporal behaviour of the temperature fields can result in the early phase of the ignition process compared to the case when all ions are neglected. This indicates the importance of detailed ion reaction models for better understanding the initial phase of ignition phenomena.

Further calculations using this model will reveal more details of the complex processes associated with spark ignition.

ACKNOWLEDGMENTS

This work was financially supported by "Deutsche Forschungsgemeinschaft", the "Fonds der Chemischen Industrie", and by the "Max–Buchner–Forschungsstiftung".

REFERENCES

[1] Thiele, M., Selle, S., Riedel, U., Warnatz, J., Maas, U., *Proceedings of the Combustion Institute* 28:1177-1185 (2000).

[2] Thiele, M., Warnatz, J., Maas, U., "2D-Simulation of Ignition Induced by electrical Discharges", SAE Report No. 99011178, (1999).

[3] Hirschfelder, J.O., Curtiss, C.F., Bird, R.B., *Molecular Theory of Gases and Liquids*, John Wiley & Sons, New York, 1964.

[4] Chapman, S., Cowling, T. G., *The Mathematical Theory of Non-uniform Gases*, Cambridge University Press, Cambridge, 1970.

[5] Selle, S., Riedel, U., *Annals of the New York Academy of Sciences* 891:72-80 (1999).

[6] Maly, R., Vogel, M., *Seventeenth Symposium (International) on Combustion*, The Combustion Institute, Pittsburgh, pp. 821–831 (1987).

[7] Maly, R., *Eighteenth Symposium (International) on Combustion*, The Combustion Institute, Pittsburgh, pp. 1747–1754 (1981).

[8] Pischinger, S., Heywood, J.B., "A Study of Flame Development and Engine Performance with Breakdown Ignition Systems in a Visualization Engine", SAE Report No. 880518, (1988).

[9] Agnew, W. G., Room at the piston top. Contributions of combustion sciene to engine design, Twentieth symposium (International) on Combustion/The Combustion Institute, 1–17, (2001).

[10] Pischinger, S., Heywood, J.B., "How Heat Losses to the Spark Plug Electrodes Affect Flame Kernel Development in an SI Engine", SAE Report No. 900021, (1990).

[11] Ko, Y., Anderson, R.W., ”Electrode Heat Transfer During Spark Ignition”, SAE Report No. 892083, (1989).

[12] Akram, M., *AIAA J.* 34(9):1835-1842 (1996).

[13] Kravchik, T., Sher, E., Heywood, J.B., *Combust. Sci. and Technol.* 108:1-30 (1995).

[14] Akindelle, O. O., Bradley, D., Mak, P.W., McMahon, M., *Combust. Flame* 47:129–155 (1982).

[15] Schäfer, M., *Thesis*, Institut für Physikalische Elektronik, Universität Stuttgart (1997).

[16] Maas, U., Warnatz, J., *IMPACT Comput. Sci. Eng.* 1:394–420 (1989).

[17] Jackson, J.D., *Classical Electrodynamics*, John Wiley & Sons, New York, 1975.

[18] Thiele, M., ”Simulation von Funkenzündungen”, Ph.D. Thesis, Interdisziplinäres Zentrum für wissenschaftliches Rechnen, University of Heidelberg, (1999)

[19] Karbach, V., *Masterthesis*, Institut für Wissenschaftliches Rechnen, Universität Heidelberg (1997).

[20] Ern, A., Giovangigli, V., *J. Comp. Phys.* 120:105-116 (1995).

[21] Bird, R.B. and Stewart, W.E. and Lightfoot, E.N., *Transport Phenomena*, John Wiley & Sons, New York, 1960.

[22] Deuflhard, Hairer E., Zugck, J., ”One-Step and Extrapolation Methods for Differential/Algebraical Systems”, Universität Heidelberg, SFB 123 Report No. 318, (1985).